

# SARS-CoV-2 Spike Protein Induces Oxidative Stress and Senescence in Mouse and Human Lung

JOEL S. GREENBERGER<sup>1</sup>, WEN HOU<sup>1</sup>, DONNA SHIELDS<sup>1</sup>, RENEE FISHER<sup>1</sup>,  
MICHAEL W. EPPERLY<sup>1</sup>, INDERPAL SARKARIA<sup>2</sup>, PETER WIPF<sup>3</sup> and HONG WANG<sup>4</sup>

<sup>1</sup>Department of Radiation Oncology, UPMC Hillman Cancer Center, Pittsburgh, PA, U.S.A.;

<sup>2</sup>Department of Thoracic Surgery, UPMC-Shadyside, Pittsburgh, PA, U.S.A.;

<sup>3</sup>Department of Chemistry, University of Pittsburgh, Pittsburgh, PA, U.S.A.;

<sup>4</sup>Department of Biostatistics, University of Pittsburgh, Pittsburgh, PA, U.S.A.

**Abstract.** *Background/Aim:* There is concern that people who had COVID-19 will develop pulmonary fibrosis. Using mouse models, we compared pulmonary inflammation following injection of the spike protein of SARS-CoV-2 (COVID-19) to radiation-induced inflammation to demonstrate similarities between the two models. SARS-CoV-2 (COVID-19) induces inflammatory cytokines and stress responses, which are also common to ionizing irradiation-induced acute pulmonary damage. Cellular senescence, which is a late effect following exposure to SARS-CoV-2 as well as radiation, was investigated. *Materials and Methods:* We evaluated the effect of SARS-CoV-2 spike protein compared to ionizing irradiation in K18-hACE2 mouse lung, human lung cell lines, and in freshly explanted human lung. We measured reactive oxygen species, DNA double-strand breaks, stimulation of transforming growth factor-beta pathways, and cellular senescence following exposure to SARS-CoV-2 spike protein, irradiation or SARS-CoV-2 and irradiation. We also measured the effects of the antioxidant radiation mitigator MMS350 following irradiation or exposure to SARS-CoV-2. *Results:* SARS-CoV-2 spike protein induced reactive oxygen species, DNA double-strand breaks, transforming growth factor- $\beta$  signaling pathways, and

senescence, which were exacerbated by prior or subsequent ionizing irradiation. The water-soluble radiation countermeasure, MMS350, reduced spike protein-induced changes. *Conclusion:* In both the SARS-CoV-2 and the irradiation mouse models, similar responses were seen indicating that irradiation or exposure to SARS-CoV-2 virus may lead to similar lung diseases such as pulmonary fibrosis. Combination of irradiation and SARS-CoV-2 may result in a more severe case of pulmonary fibrosis. Cellular senescence may explain some of the late effects of exposure to SARS-CoV-2 spike protein and to ionizing irradiation.

The global pandemic caused by SARS-CoV-2 (COVID-19) resulted in acute respiratory distress syndrome (ARDS) with clinical presentations (1-16) that were like those of ionizing irradiation-induced pneumonitis and fibrosis (17, 18). Similarities between COVID-19 and ionizing irradiation-induced changes in the lung have led to speculation that some biomolecular and biochemical responses may involve common pathways (19, 20). Prior research demonstrated potential additive or synergistic deleterious effects of pulmonary virus infections with damage induced by pre-existing lung diseases, and with ionizing irradiation-induced lung damage (21- 25). There is emerging evidence that late-stage effects of COVID-19 infection may include similar pathways (26-35) leading to pulmonary fibrosis (34-42). Lung fibrosis may involve several different initiating steps (42-55). There is recent evidence that the late-stage effects of both COVID-19 and ionizing irradiation include cellular senescence in lung tissue, which may be a common step in the induction of pulmonary fibrosis after both forms of lung injury (56-61).

To establish a potential role of senescence in COVID-19-induced lung fibrosis, we took advantage of the availability of the K18-hACE2 mouse strain, which is transgenic for the human angiotensin-converting enzyme 2 (ACE2) receptor and has been demonstrated to be a useful model of COVID-

*Correspondence to:* Joel S. Greenberger, MD, FACRO, FACR, FASTRO, Professor and Chairman, Department of Radiation Oncology, UPMC Hillman Cancer Center, UPMC Cancer Pavilion, Rm. 533, 5150 Centre Avenue, Pittsburgh, PA 15232, U.S.A. Tel: +1 4126473602, Fax: +1 4126476029, e-mail: greenbergerjs@upmc.edu

**Key Words:** Reactive oxygen species, COVID-19, spike protein, oxidative stress.



This article is an open access article distributed under the terms and conditions of the Creative Commons Attribution (CC BY-NC-ND) 4.0 international license (<https://creativecommons.org/licenses/by-nc-nd/4.0/>).

19-induced pulmonary damage (62). In the present studies, we prepared explanted lung single-cell suspensions from these mice and compared them to C57BL/6J control mice. We tested the effect of the addition of SARS-CoV-2 spike protein to each cell suspension, and measured the induction of stress response and inflammatory cytokine pathways that are known to be activated by ionizing irradiation (63-67). We also quantitated the effects of SARS-CoV-2 spike protein with human lung cell lines and explanted single cell suspensions of freshly explanted mouse lung tissues, and human lung tissues. The data suggest caution in the use of lung irradiation in patients with COVID-19 presenting with ARDS as a potential therapeutic to reduce the numbers of inflammatory cells and reduce the cytokine storm associated with COVID-19-induced ARDS (20).

## Materials and Methods

**Experimental design.** We demonstrated that both COVID-19 infection and irradiation both of which result in the development of pulmonary fibrosis have the same initial steps. To demonstrate the similarities between the two, we performed *in-vitro* studies using murine bone marrow stromal cell lines and lung epithelium cells from K18-hACE2 or C57BL/6 mice. We also used normal human epithelial cells, as well as human cancer cell lines. For these studies, the cells were assigned to four main groups including i) control, nontreated cells ii) cells treated with 50 µg/ml SARS-CoV-2 spike protein for 24 h, iii) cells irradiated to 5 Gy, and iv) cells treated with 50 µg/ml SARS-CoV-2 spike protein for 24 h and then irradiated to 5 Gy. Twenty-four hours after the addition of SARS-CoV-2 spike protein or after irradiation, the cells were analyzed for expression of hACE2 protein, binding of SARS-CoV-2 spike protein, production of reactive oxygen species (ROS), DNA strand breaks, and senescence. The inhibition of hACE2 protein using hACE2 siRNA and stimulation of transforming growth factor (TGF)-β pathways was performed.

**Mice and animal care.** K18-hACE2 and C57BL/6NTac mice were obtained from Jackson Laboratories (Bar Harbor, ME, USA), and Taconic Biosciences (Germantown, NY, USA), respectively. K18-hACE2 mice were bred in the Hillman Animal Facility at the University of Pittsburgh. Animals were housed four per cage and maintained on standard laboratory chow and deionized water. All animal protocols were approved by the University of Pittsburgh Institutional Animal Care and Use Committee (IACUC). The PHS Assurance Number for the University of Pittsburgh IACUC is D16-00118.

**SARS-CoV-2 spike protein.** This protein was obtained from RayBiotech (catalog #230-01102; Norcross, GA, USA). The protein has a histidine (His) tag at the N-terminal end. It was dissolved in sterile phosphate-buffered saline (PBS) at 5 µg/ml and used *in vitro* at 0.50 µg/ml.

**Human and mouse cell lines.** The human lung epithelial cancer cell line H460 and IB3 have been previously described (68). The tumor cell line was passaged *in vitro* and maintained in a subconfluent condition in Dulbecco's modified Eagle's medium supplemented

with 10% fetal calf serum. Mouse cell lines were established according to published methods from long-term bone marrow cultures (59). Bone marrow was flushed from the femurs of K18ACE2<sup>+/−</sup> (Jackson Laboratories) and C57BL/6NTac control mice into T25 tissue culture flasks containing Fisher's medium (ThermoFisher Scientific, Waltham, MA, USA) containing 20% horse serum, penicillin-streptomycin (Pen-Strep; Millipore Sigma, Danvers, MA, USA) and 10<sup>−6</sup>M hydrocortisone hemi-succinate (Millipore Sigma). At 3 to 4 weeks after establishing the cultures, the horse serum was changed to fetal calf serum and the hydrocortisone removed. Each week the nonadherent cells were removed and placed in Fisher's medium supplemented with recombinant murine interleukin-3 (IL-3; #213-13; Peprotech, Cranbury, NJ, USA). Once the nonadherent cell production was completed, the stromal cell line was isolated.

**Preparation of single-cell suspensions.** Mouse lung explants: Lungs from female K18-hACE2 and C57BL/6NTac mice (30-33 g adult) were excised according to previous publications and a single-cell suspension prepared as described therein (66, 67). Briefly, the lungs were minced, and digested with collagenase A. The cells were maintained in Dulbecco's modified Eagle's medium supplemented with 15% fetal bovine serum and antibiotics with a final concentration of 200 mM L-glutamine, and Pen-Strep (10,000 U/ml penicillin and 10,000 U/ml streptomycin) (69, 70). Fresh cell explants were studied in all assays.

**Human lung explants.** Fresh human lung specimens were obtained from two individual patients at the time of pulmonary segment resection for non-small-cell lung cancer. The samples were identified by an honest broker according to guidelines established by the University of Pittsburgh Institutional Review Board. The acquisition of the tissue samples was obtained using Institutional Review Board-approved study 19080204. Normal lung specimens from the margin (1 cm or greater outside tumor margin) were excised, and 10 g of tissue from each specimen were prepared in single-cell suspensions according to a previous publication (69) and cultured in medium as described above for mouse cells. Each human lung specimen was studied at the time of acquiring the fresh explant.

**Expression of ACE2 protein and binding of SARS-CoV-2 spike protein.** Mouse bone marrow cells and lung epithelial cells were isolated from K18-hACE2 and C57BL/6 mice as described above. The cells were treated with SARS-CoV-2 spike protein and 5 Gy irradiation as described above. Twenty-four hours later, the cells were fixed in 3.7% paraformaldehyde and incubated with antibodies to human ACE2 or spike protein (ab15348 or ab18184; Abcam, Cambridge, MA, USA) for 1 h at 37°C. The cells were washed with PBS, and incubated with goat-anti-mouse IgG (ab150113; Abcam) or goat anti-rabbit IgG (ab15007; Abcam) for 30 min at 37°C. The cells were then washed and photographed.

**Inhibition of hACE2 protein using hACE2 siRNA.** H460 human epithelial lung cancer cell line was grown to 70% confluence and transfected with ACE2 siRNA or control siRNA (ThermoFisher Scientific) using Lipofectamine 3000 reagent (ThermoFisher Scientific). Twenty-four hours later the transfected cells were grown in medium containing puromycin (4 µg/ml). The culture media was replaced with fresh media containing puromycin to remove dead cells. When the puromycin-resistant cells reached 80% confluency,

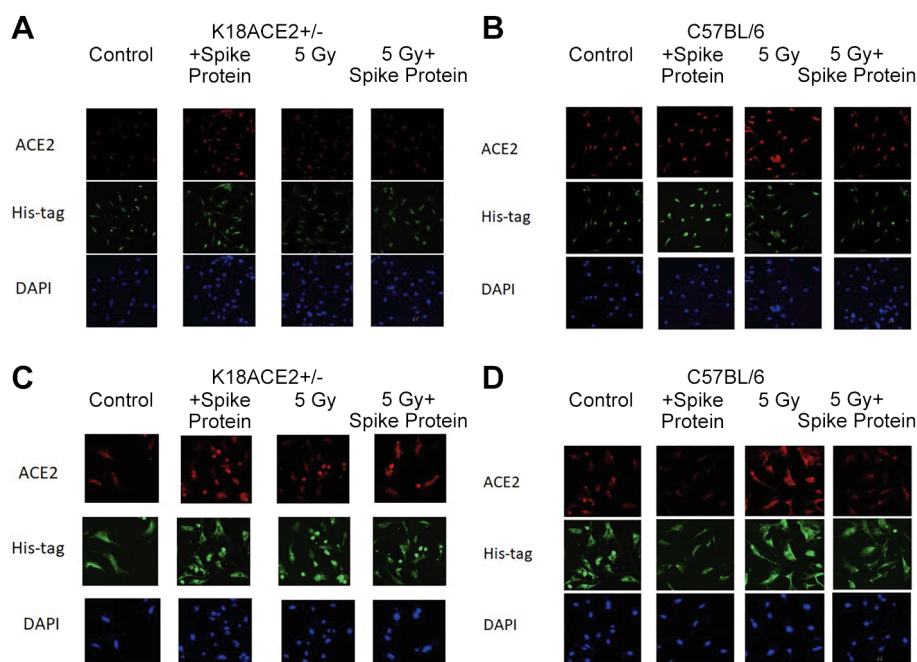


Figure 1. Angiotensin-converting enzyme 2 (ACE2) expression detected in K18-hACE2 mouse lung tissues following incubation with SARS-CoV-2 spike protein with/without irradiation. K18-hACE2 and C57BL/6 bone marrow stromal cells (A and B) or lung endothelial cells (C and D) were incubated with spike protein alone or irradiated to 5 Gy or treated with spike protein with irradiation. Twenty-four hours later, the cells were fixed and stained using antibodies for human ACE2 protein, or spike protein. Bone marrow stromal cells from either mouse strain or C57BL/6 lung endothelial cells did not express ACE2 protein or bind the spike protein (A, B and D). K18-hACE2 lung endothelial cells incubated with spike protein, 5 Gy, 5 Gy + spike protein had increased ACE2 expression with increased SARS-Cov-2 spike protein binding (C)

reverse transcriptase-polymerase chain reaction using primers specific for ACE2 or control siRNA was performed to demonstrate that the cells were successfully transfected. Forty-eight hours later, 0.50  $\mu\text{g/ml}$  of SARS-CoV-2 spike protein containing a His tag were added. The cells were stained 18 h later with an anti-ACE2 or anti-His antibody, and 4',6-diamidino-2-phenylindole (Millipore Sigma) for the nuclear DNA and observed under a fluorescence microscope.

**Assay for reactive oxygen species (ROS).** Single-cell suspensions of fresh human lung were made as described above. Production of ROS was determined using a Cellular ROS/Superoxide Detection Assay Kit (#139476; Abcam, Waltham, MA, USA). Single human lung cells were plated in 96-well plates and grown to 70 to 80% confluency. The wells were divided into four groups and treated as described in the experimental design. One hour later, the cells were washed with medium and 100  $\mu\text{l}$  of ROS/Superoxide Detection solution was added to each well. One hour later, the wells were read using a fluorescent spectrophotometer (66, 67).

**Assay for DNA double-strand breaks.** DNA double-strand breaks were measured by using an assay for binding of gamma H2AX DNA strand breaks in individual cells using a Gamma H2A.X binding kit (ab242296; Abcam) as previously described (66, 67, 70). Single human lung cells obtained as described above were plated in 96-well plates and grown to 70 to 80% confluence. The wells were then divided into four groups and treated as described in the experimental design. The cells were then washed and fixed in 100  $\mu\text{l}$  of 3.7% paraformaldehyde. The cells were washed with 200  $\mu\text{l}$  of PBS, 100  $\mu\text{l}$

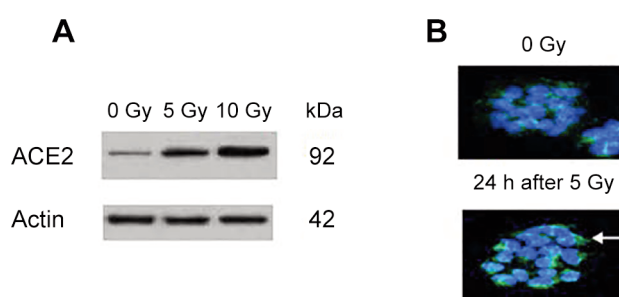


Figure 2. Expression of angiotensin-converting enzyme 2 (ACE2) on human H460 lung carcinoma cells. Irradiation to 5 Gy or 10 Gy induces expression of the SARS-CoV-2 ACE2 receptor in human epithelial (H460 lung carcinoma) cells as detected by western blot (A) and on cell surface as shown by antibody to ACE2 (B) (green, white arrow). Similar results were observed with IB3 cells and freshly explanted human lung cells ( $\times 200$ ).

of 100% methanol was added for 10 min at 4°C and washed with 200  $\mu\text{l}$  of PBS. Blocking buffer was added for 30 min at room temperature, following aspiration of the blocking buffer, an anti-phospho-H2AX antibody was added and incubated for 1 h at room temperature while shaking on an orbital shaker. The cells were washed, and a fluorescein isothiocyanate-conjugated antibody as provided in the Gamma-H2A.X kit was added and incubated for 1 h at room temperature. The cells

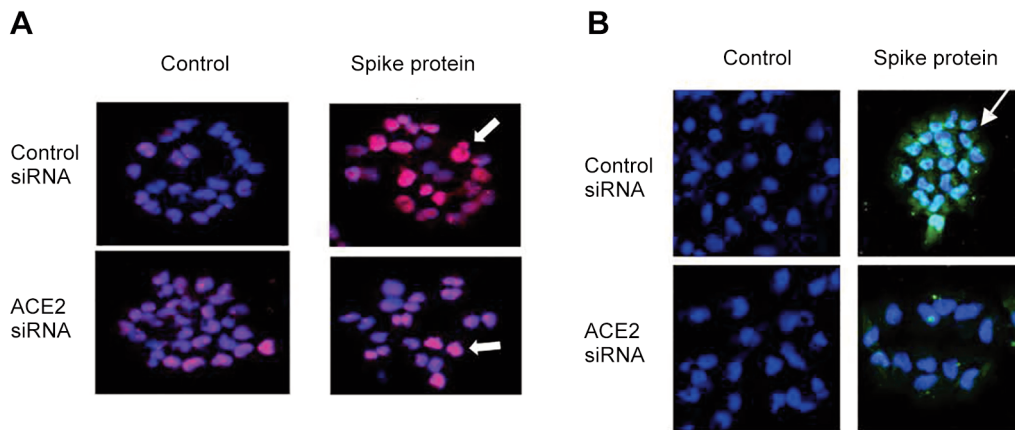


Figure 3. Angiotensin-converting enzyme 2 small interfering RNA (ACE2 siRNA) reduces expression of ACE2 protein and binding of SARS-Cov-2 spike protein to the cell surface of H460 human lung cancer cells. The H460 human epithelial lung cancer cell line was transfected with ACE2 siRNA or control siRNA. Forty-eight hours later, 0.50 µg/ml of SARS-CoV-2 spike protein containing a His tag were added. The cells were stained 18 h later with an anti-ACE2 or anti-His, and 4',6-diamidino-2-phenylindole for the nucleus. H460 cells treated with ACE2 siRNA had a decreased expression of ACE2 protein (A). ACE2 siRNA also reduced binding of spike protein to the cell surface (B). Pink color is antibody to the ACE2 protein (white arrow). Green color is antibody to the His tag on SARS-CoV-2 spike protein (white arrow) (×100).

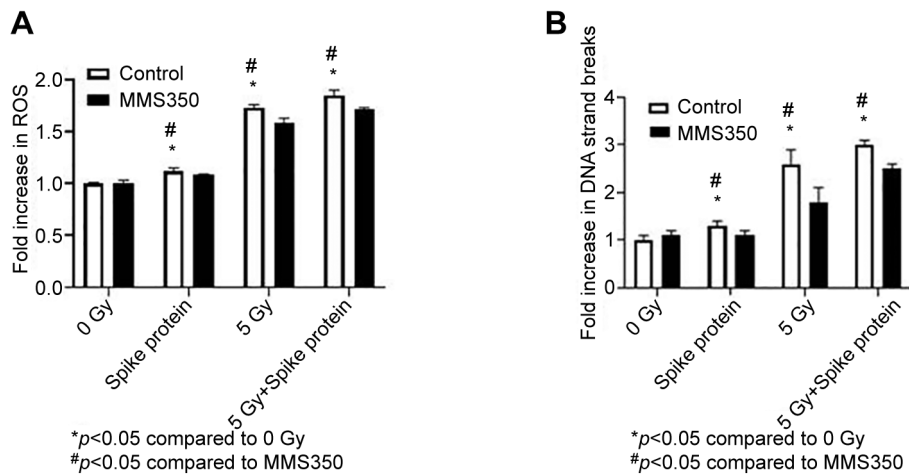


Figure 4. SARS-CoV-2 spike protein induces reactive oxygen species (ROS), and DNA double-strand breaks (measured by H2AX) in human lung cells. Single-cell suspension of freshly explanted normal human lung cells (A-B) were seeded at 10<sup>4</sup> cells per well into 96-well plates. Half of the culture wells were incubated with the antioxidant MMS350 (400 µM) one hour before addition of spike protein (0.50 µg/ml), 5 Gy irradiation or both spike protein plus 5 Gy. One hour later, cells were assayed for ROS (A) and DNA double-strand breaks (B). For the statistical analysis, analysis of variance followed by a Student's t-test were used. ROS increased in human lung cells under all conditions and was reduced when cells were incubated in MMS350. DNA double-strand breaks in human lung samples (n=4) were increased under all treatments but were reduced when the cells were treated with MMS350. Significantly different at p<0.05 vs. \*0 Gy, #MMS350.

were washed for 5 min using 200 µl of PBS and fluorescence measured using a fluorescent spectrophotometer.

**Western analysis of transforming growth factor-β signaling pathways.** The assays for five different TGF-β signaling pathways have been described in detail previously (71). These assays were carried out on protein extracted from aliquots of human cell preparations. A 100 mg piece of normal human lung tissue was placed in 1 ml of cell lysis buffer in a round test tube and homogenized using a Polytron PT3000

(Brinkman, Inc., Riverview, FL, USA). The lung samples were placed on ice for 2 h, transferred to a 1.5-ml Eppendorf tube, centrifuged in a microcentrifuge for 15 min at 17,960 ×g at 4°C, and then the supernatant was transferred to a new Eppendorf tube and stored on ice. The protein concentration was determined using Bio-Rad Protein Assay Dye Reagent Concentrate (Bio-Rad, Laboratories, Hercules, CA, USA). The protein samples were added to 4X Loading Buffer (Bio-Rad) with 10% 2-mercaptoethanol, vortexed and heat at 95-100°C for 5 min.

The samples were then loaded onto 4-12% Bis-Tris Criterion XT Precast Gels (Bio-Rad) at 145 V for 70 min using XT MES as the running buffer (Bio-Rad). The proteins were transferred to polyvinylidene difluoride membranes (Bio-Rad) at 0.45 A for 90 min using Tris/Glycine buffer (Bio-Rad) with an ice block. Nonspecific binding was blocked by incubating the membrane in 5% nonfat milk for 30 min. Reagents used included antibodies to the following: phospho-mothers against decapentaplegic (SMAD3) and phospho-cytokinin specific-binding protein (p38) (9523 and 9212; Cell Signaling Technology, Danvers, MA, USA), phosphorylated extracellular signal-regulated kinase (p-ERK) and c-Jun N-terminal kinase (p-JNK), as well as actin (sc-7383, sc-6254 and sc-8432, respectively; Santa Cruz Biotechnology Inc., Dallas, TX, USA), phospho-ribosomal s6 kinase (S6K) and phospho-p21 activated kinase (PAK) (ab308331 and ab51244, respectively; Abcam). The loading control was anti-mouse monoclonal antibody to glyceraldehyde 3-phosphate dehydrogenase (#5174; Cell Signaling Technology). The western blots were left in 5% nonfat milk overnight at 4°C and then washed three times with TBS (Bio-Rad) for 5 min. The secondary antibody [either goat anti-rabbit IgG-horseradish peroxidase (HRP) (sc2004), goat anti-mouse IgG-HRP (sc2005), or donkey anti-goat IgG-HRP (sc2020); all from Santa Cruz Biotechnology] was diluted 1:10,000 in 5% nonfat milk, incubated with the membrane for 1 h at room temperature, and washed three times with TBS for 5 min. The proteins were detected using SuperSignal™ West Pico PLUS Chemiluminescent Substrate (Thermo Fisher, Pittsburgh, PA, USA). Western blot quantification was performed using LabWorks™ Management System (Lablogics, Inc., Mission Viejo, CA, USA).

**Assay of cellular senescence.** Histochemical staining for  $\beta$ -galactosidase was used to determine senescence according to a previous publication (61). Freshly isolated human lung cells were plated at  $10^6$  cells per well in T25 tissue culture flasks. When the flasks reached 50% confluence, the cells were treated with SARS-CoV-2 spike protein, 5 Gy irradiation or spike protein plus irradiation. Oxetane-substituted sulfoxide (MMS350, prepared in the laboratory of Peter Wifp, PhD at the University of Pittsburgh) (400  $\mu$ M) was added to half of the wells of each group 1 h before the addition of SARS-CoV-2 spike protein or irradiation. Forty-eight hours later, the cells were stained for expression of  $\beta$ -galactosidase using a Senescence  $\beta$ -Galactosidase Staining Kit (#9860; Cell Signaling Technology). The cells were washed with PBS, fixed with a 1X fixative solution for 10 to 15 min, rinsed twice with PBS and then stained with  $\beta$ -Galactosidase Staining solution. The cells were incubated at 37°C at least overnight. The cells were observed under a microscope for blue staining which is indicative of senescent cells expressing  $\beta$ -galactosidase.

**In-vitro irradiation of fresh cell explants.** Cells in culture were irradiated using a cesium-137 gamma cell irradiator at a dose rate of 600 cGy per minute according to published methods (61). Cells were treated in monolayer, and immediately after irradiation were harvested for assays. For some experiments, SARS-CoV-2 spike protein was added prior to irradiation or immediately after irradiation.

**Statistical analysis.** The different groups were first tested with analysis of variance test. When statistical differences were found, individual groups were analyzed with Student's *t*-test (17, 64-65). Statistical differences were found when the *p*-value was less than 0.05.

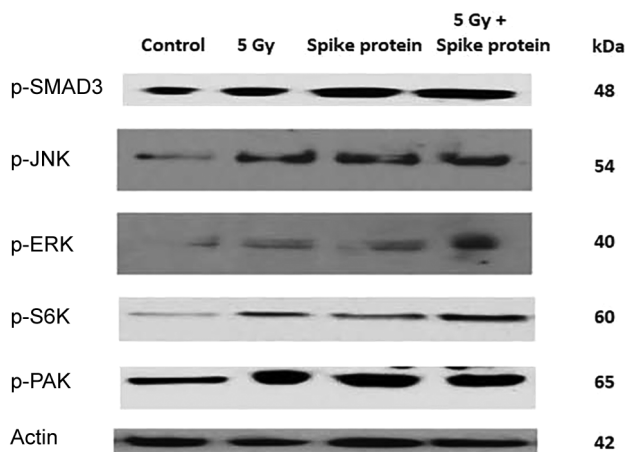


Figure 5. SARS-CoV-2 spike protein induces mothers against decapentaplegic homolog 3 (SMAD3)-dependent and four other SMAD3-independent transforming growth factor-beta (TGF- $\beta$ ) signaling pathways in IB3 human lung epithelial cells. Western blot analysis was performed on the IB3 human lung cell line at 96 h following treatment with SARS-CoV-2 spike protein (0.50  $\mu$ g/ml), 5 Gy irradiation, or both 5 Gy and spike protein. Blots were stained with antibodies to SMAD3, phosphorylated extracellular signal-regulated kinases (p-ERK), c-Jun N-terminal kinase (p-JNK), ribosomal S6 kinase (p-S6K), and p21 (RAC1) activated kinase (p-PAK) (representing each of the four SMAD3-independent signaling pathways) (70) and standardized to actin. Irradiation with 5 Gy, spike protein, or both 5 Gy and spike protein increased signaling by all five TGF- $\beta$  signaling pathways compared to untreated control cells.

## Results

**SARS-CoV-2 spike protein binds to ACE2 receptor-positive K18-hACE2 mouse lung cells similarly to freshly excised human lung cells.** We confirmed that K18-hACE2 mice transgenic for human ACE2 demonstrated the presence of ACE2 receptors and binding of labeled SARS-CoV-2 spike protein in lung tissue, but not in bone marrow, as shown in Figure 1. The explanted K18-hACE2 mouse lung demonstrated binding of SARS-CoV-2 spike protein to ACE2 receptor. In contrast, C57BL/6J mouse lung tissue did not demonstrate ACE2 receptor or SARS-CoV-2 spike protein binding (Figure 1).

Freshly explanted single-cell suspensions of human lung tissue demonstrated significant levels of cell surface ACE2 receptor and SARS-CoV-2 spike protein binding (Figure 2, Figure 3, and Figure 4).

**SARS-CoV-2 spike protein induces ROS and DNA double-strand breaks in single-cell suspensions of human lung.** We compared SARS-CoV-2 spike protein-induced ROS and DNA double-strand breaks with those induced by ionizing irradiation. As shown in Figure 4A, human lung cells demonstrated significant ROS by fluorochrome assay *in vitro*. As shown in

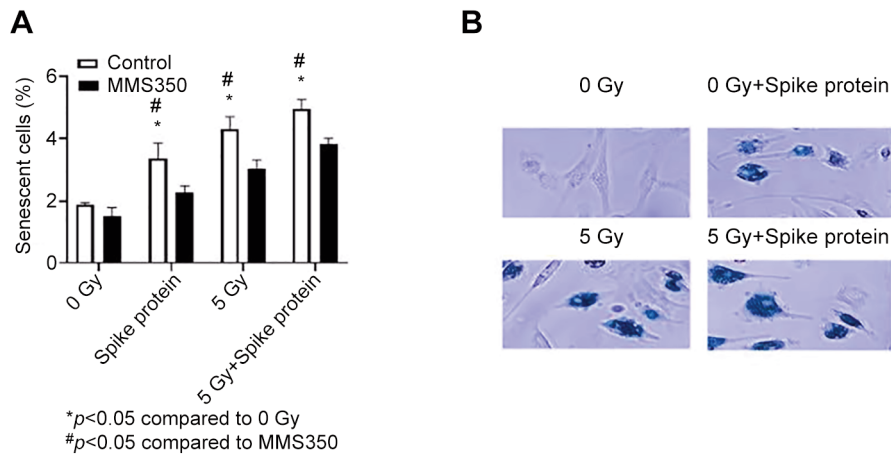


Figure 6. SARS-Cov-2 spike protein stimulates senescence in human lung cells. Fresh human lung cells were seeded into T25 flasks at  $10^6$  cells per flask, and when 50% confluent, spike protein was then added (0.50  $\mu\text{g/ml}$ ). Other flasks were irradiated to 5 Gy or treated with both spike protein and 5 Gy 24 h after addition of spike protein. To half of the flasks in each group, antioxidant radiation mitigator MMS350 (400  $\mu\text{M}$ ) was added to the cells, 1 hour before addition of spike protein to the flasks. Forty-eight hours after irradiation, cells were stained for  $\beta$ -galactosidase. For scoring senescent cells, five microscopic fields of 1,500 cells were counted, and the percentage of senescent cells was determined with ANOVA followed by Student's t-test to determine statistical significance (A). The increase in senescent cells was detected following the addition of spike protein, 5 Gy, or 5 Gy plus spike protein, and their number was reduced by MMS350 (61, 71). (B) Photos of representative fields scoring senescent cells (blue) ( $\times 100$ ). Significantly different at  $p < 0.05$  vs. \*0 Gy, #MMS350.

Figure 4B, DNA double-strand breaks as measured by P-H2AX were induced by SARS-CoV-2 spike protein and ionizing irradiation *in vitro*. We tested the effect of an antioxidant by using an ionizing irradiation countermeasure, the water-soluble dimethyl sulfoxide-analog, MMS350 (61, 72) (Figure 4B), with respect to SARS-CoV-2 spike protein-induced ROS and DNA double-strand breaks. The results, which are shown in Figure 4 demonstrate that MMS350 caused a significant decrease in both the ionizing irradiation-induced and the SARS-CoV-2 spike protein-induced elevation of these biomarkers.

*SARS-CoV-2 spike protein induces TGF- $\beta$  signaling pathways in human lung cells in-vitro.* Human lung specimens were treated with SARS-CoV-2 spike protein or irradiation, as described in the Materials and Methods, and then analyzed for each of five TGF- $\beta$  signaling pathways (71). The results demonstrate that both SARS-CoV-2 spike protein and ionizing irradiation induced TGF- $\beta$  signaling pathways *in vitro* (Figure 5).

*SARS-CoV-2 spike protein induces senescence in human lung cells in vitro.* We utilized a standard assay for senescence, the expression of  $\beta$ -galactosidase in cells in culture (Figure 6). Human lung samples were treated with SARS-CoV-2 spike protein or ionizing irradiation. Cells were stained for  $\beta$ -galactosidase (61), which was increased by both spike protein and irradiation (Figure 6B) and reduced by MMS350 (Figure 6B).

## Discussion

Lung fibrosis in COVID-19 survivors is clearly a component of the late effects of COVID-19 disease, which is appearing in increasing numbers of patients each year (39-48, 54, 55). While the application of vaccines has significantly reduced the incidence of acute disease from SARS-CoV-2, the increase in clinical presentation of late effects of COVID-19 is alarming.

There is evidence that cellular senescence precedes fibrosis in several etiologies of lung fibrosis. Prominent in the pathophysiology of radiation-induced pulmonary fibrosis (RIPF) and silicosis (also called Black Lung Disease or Miner's Lung) is the detection of senescent cells in the lungs prior to fibrosis (58-60).

Senescent cells have recently been shown to produce FGR proto-oncogene, an Src family tyrosine kinase (FGR), which is elevated in senescent cells significantly prior to the detection of histological biomarkers of fibrosis in the RIPF model (59, 60).

FGR is a component of a group of proteins produced by senescent cells called senescence-associated secretory proteins. Recent study demonstrated that senescent cells show up-regulation of FGR induced by irradiation or intrapulmonary injection of silica and, specifically, phosphorylation of FGR (59). Administration of an inhibitor of FGR phosphorylation (TL02-59) to mice in the model of RIPF or silicosis prevented activation of FGR, and significantly reduced lung fibrosis (60). There is also

evidence that FGR is involved in the early phases of idiopathic pulmonary fibrosis (IPF) in humans. This disease represents a collection of clinical presentations of progressive pulmonary fibrosis, in many cases, of unknown cause. Clinical trials with novel drugs, approved by the Food and Drug Administration, to treat IPF have not yet specifically targeted FGR but rather have focused on limiting ROS or other inflammatory biomarkers of the late pulmonary response to potentially toxic factors in the environment. The cause and an effective treatment of IPF are still unknown.

The COVID-19 pandemic has provided yet another example of the potential for elevated levels of senescent cells to cause pulmonary fibrosis. The present study demonstrated that, when added to lung cells or tissues from mice or humans, SARS-CoV-2 spike protein induces both senescence and profibrotic TGF- $\beta$  signaling. The components of the senescence-associated secretory proteins in senescent cells induced by SARS-CoV-2 spike protein are not known. As more cases of late fibrosis appear in COVID-19 survivors, there will be an opportunity to study the senescent cells in lung specimens and in patients to determine whether FGR or other specific tyrosine kinases are involved in the earliest stages of the induction of pulmonary fibrosis.

The molecular mechanism of action of the SARS-CoV-2 virus with respect to induction of the ARDS is similar not only to that of other infectious agents, but also to that of ionizing irradiation-induced acute lung injury. There are increasing numbers of reports of the late-stage effects of COVID-19 in patients recovering from ARDS (1-4), and the presentation of these effects in the lung is similar to those caused by ionizing irradiation, including radiation fibrosis (15-20, 66, 69-70). These concerns now suggest caution in the use of standard protocols of regular clinical radiotherapy in patients who have recovered from ARDS caused by COVID-19 (20). There is concern for possible additive or synergistic effects of late COVID-19 effects and ionizing irradiation in the human lung.

In the present study, we questioned whether cellular senescence was a possible mechanism of induction of late-stage COVID-19-induced lung damage, namely, fibrosis. Senescence is known to lead to the induction of biomarkers of lung fibrosis including FGR (59, 60). We tested whether known parameters of ionizing irradiation damage to mouse and human lung tissue *in vitro* were also detected following exposure to SARS-CoV-2 spike protein. The results demonstrate that the spike protein does indeed induce biomolecular and biochemical changes in both K18-hACE2 mouse, and human lung specimens *in vitro*, including the induction of ROS, DNA double-strand breaks (measured by H2AX), induction of TGF- $\beta$  signaling pathways associated with acute induction of inflammatory cytokines, and cellular senescence. We discovered that there is a potential additive effect of irradiation together with SARS-CoV-2 spike protein

exposure *in vitro*. The results also show that a small-molecule radiation countermeasure, the antioxidant molecule MMS350, reduced several parameters of SARS-CoV-2 spike protein-induced changes in human lung tissue *in vitro*.

We observed that SARS-CoV-2 spike protein (73-75) induced senescence in human lung cells *in vitro*. Recent evidence suggests that senescent cells may be involved in elaborating pro-fibrotic cytokines associated with radiation pulmonary fibrosis (76). If patients recovering from COVID-19-induced ARDS are at risk for increased numbers of senescent cells in the lung, and if senescent cells caused by COVID-19 contribute to pulmonary fibrosis, then the addition of ionizing irradiation to the care of these patients merits increased caution (77, 78). The use of senolytic drugs as a therapeutic for patients developing fibrosis from prior SARS-CoV-2 infection may also be of potential value (68, 79-86). Further studies will be required in mouse models of COVID-19, including K18-hACE2 mice, to determine the kinetics of induction and the duration of deleterious changes induced by SARS-CoV-2 spike protein *in vivo*.

## Conflicts of Interest

None of the Authors have any conflicts of interest.

## Authors' Contributions

W.H. carried out immunohistochemistry; D.S. carried out culture experiments, preparation of single-cell suspensions, and preparation of cells for immunohistochemistry, R.F. harvested mouse tissues and maintained animals for all studies; M.W.E. oversaw all experiments with human and mouse tissues in the laboratory and edited the article; I.S. provided normal tissue specimens of human lung from Department of Thoracic Surgery protocols; P.W. provided MMS350 antioxidant drug for experiments; H.W. carried out statistical analysis; J.S.G. planned experiments, wrote, and edited the article.

## Acknowledgements

This study was supported by NIAID/NIH grant U19-AI068021. Research reported in this publication was supported by the National Cancer Institute of the National Institutes of Health under Award Number P30CA047904.

## References

- 1 Wang J, Wang BJ, Yang JC, Wang MY, Chen C, Luo GX, He WF: [Research advances in the mechanism of pulmonary fibrosis induced by coronavirus disease 2019 and the corresponding therapeutic measures]. *Zhonghua Shao Shang Za Zhi* 36(8): 691-697, 2020. DOI: 10.3760/cma.j.cn501120-20200307-00132
- 2 Conti P, Ronconi G, Caraffa A, Gallenga CE, Ross R, Frydas I, Kritas SK: Induction of pro-inflammatory cytokines (IL-1 and IL-6) and lung inflammation by Coronavirus-19 (COVI-19 or SARS-CoV-2): anti-inflammatory strategies. *J Biol Regul Homeost Agents* 34(2): 327-331, 2020. DOI: 10.23812/CONTI-E

- 3 Kim J, Yang YL, Jeong Y, Jang YS: Middle East respiratory syndrome-Coronavirus infection into established hDPP4-transgenic mice accelerates lung damage *via* activation of the pro-inflammatory response and pulmonary fibrosis. *J Microbiol Biotechnol* 30(3): 427-438, 2020. DOI: 10.4014/jmb.1910.10055
- 4 Das KM, Lee EY, Singh R, Enani MA, Al Dossari K, Van Gorkom K, Larsson SG, Langer RD: Follow-up chest radiographic findings in patients with MERS-CoV after recovery. *Indian J Radiol Imaging* 27(3): 342-349, 2017. DOI: 10.4103/ijri.IJRI\_469\_16
- 5 Lin CI, Tsai CH, Sun YL, Hsieh WY, Lin YC, Chen CY, Lin CS: Instillation of particulate matter 2.5 induced acute lung injury and attenuated the injury recovery in ACE2 knockout mice. *Int J Biol Sci* 14(3): 253-265, 2018. DOI: 10.7150/ijbs.23489
- 6 He L, Ding Y, Zhang Q, Che X, He Y, Shen H, Wang H, Li Z, Zhao L, Geng J, Deng Y, Yang L, Li J, Cai J, Qiu L, Wen K, Xu X, Jiang S: Expression of elevated levels of pro-inflammatory cytokines in SARS-CoV-infected ACE2+ cells in SARS patients: relation to the acute lung injury and pathogenesis of SARS. *J Pathol* 210(3): 288-297, 2006. DOI: 10.1002/path.2067
- 7 Rogers CJ, Lukaszewicz AI, Yamada-Hanff J, Micewicz ED, Ratikan JA, Starbird MA, Miller TA, Nguyen C, Lee JT, Olafsen T, Iwamoto KS, McBride WH, Schaeue D, Menon N: Identification of miRNA signatures associated with radiation-induced late lung injury in mice. *PLoS One* 15(5): e0232411, 2020. DOI: 10.1371/journal.pone.0232411
- 8 Ziegler CGK, Allon SJ, Nyquist SK, Mbanjo IM, Miao VN, Tzouanas CN, Cao Y, Yousif AS, Bals J, Hauser BM, Feldman J, Muus C, Wadsworth MH 2nd, Kazer SW, Hughes TK, Doran B, Gatter GJ, Vukovic M, Taliaferro F, Mead BE, Guo Z, Wang JP, Gras D, Plaisant M, Ansari M, Angelidis I, Adler H, Sucre JMS, Taylor CJ, Lin B, Waghray A, Mitsialis V, Dwyer DF, Buchheit KM, Boyce JA, Barrett NA, Laidlaw TM, Carroll SL, Colonna L, Tkachev V, Peterson CW, Yu A, Zheng HB, Gideon HP, Winchell CG, Lin PL, Bingle CD, Snapper SB, Kropski JA, Theis FJ, Schiller HB, Zaragosi LE, Barbry P, Leslie A, Kiem HP, Flynn JL, Fortune SM, Berger B, Finberg RW, Kean LS, Garber M, Schmidt AG, Lingwood D, Shalek AK, Ordovas-Montanes J, HCA Lung Biological Network: SARS-CoV-2 receptor ACE2 is an interferon-stimulated gene in human airway epithelial cells and is detected in specific cell subsets across tissues. *Cell* 181(5): 1016-1035.e19, 2020. DOI: 10.1016/j.cell.2020.04.035
- 9 van der Veen SJ, Ghobadi G, de Boer RA, Faber H, Cannon MV, Nagle PW, Brandenburg S, Langendijk JA, van Luijk P, Coppes RP: ACE inhibition attenuates radiation-induced cardiopulmonary damage. *Radiother Oncol* 114(1): 96-103, 2015. DOI: 10.1016/j.radonc.2014.11.017
- 10 Li Y, Zeng Z, Cao Y, Liu Y, Ping F, Liang M, Xue Y, Xi C, Zhou M, Jiang W: Angiotensin-converting enzyme 2 prevents lipopolysaccharide-induced rat acute lung injury *via* suppressing the ERK1/2 and NF- $\kappa$ B signaling pathways. *Sci Rep* 6: 27911, 2016. DOI: 10.1038/srep27911
- 11 Meletiadis J, Tsiodras S, Tsigotis P: Interleukin-6 blocking *vs.* JAK-STAT inhibition for prevention of lung injury in patients with COVID-19. *Infect Dis Ther* 9(4): 707-713, 2020. DOI: 10.1007/s40121-020-00326-1
- 12 Jansen J, Reimer KC, Nagai JS, Varghese FS, Overheul GJ, de Beer M, Rovers R, Daviran D, Fermin LAS, Willemsen B, Beukenboom M, Djudjaj S, von Stillfried S, van Eijk LE, Mastik M, Bulthuis M, Dunnen WD, van Goor H, Hillebrands JL, Triana SH, Alexandrov T, Timm MC, van den Berge BT, van den Broek M, Nlandu Q, Heijntert J, Bindels EMJ, Hoogenboezem RM, Moeren F, Kuppe C, Miesen P, Grünberg K, Ijzermans T, Steenbergen EJ, Czogalla J, Schreuder MF, Sommerdijk N, Akiva A, Boor P, Puelles VG, Floege J, Huber TB, COVID Moonshot consortium, van Rij RP, Costa IG, Schneider RK, Smeets B, Kramann R: SARS-CoV-2 infects the human kidney and drives fibrosis in kidney organoids. *Cell Stem Cell* 29(2): 217-231.e8, 2022. DOI: 10.1016/j.stem.2021.12.010
- 13 Katwa LC, Mendoza C, Clements M: CVD and COVID-19: Emerging roles of cardiac fibroblasts and myofibroblasts. *Cells* 11(8): 1316, 2022. DOI: 10.3390/cells11081316
- 14 Boshra MS, Abou Warda AE, Sayed MA, Elkomy MH, Alotaibi NH, Mohsen M, Sarhan RM: Effect of pirfenidone on risk of pulmonary fibrosis in COVID-19 patients experiencing cytokine storm. *Healthcare (Basel)* 10(12): 2387, 2022. DOI: 10.3390/healthcare10122387
- 15 Wu J, Chen L, Qin C, Huo F, Liang X, Yang X, Zhang K, Lin P, Liu J, Feng Z, Zhou J, Pei Z, Wang Y, Sun XX, Wang K, Geng J, Zheng Z, Fu X, Liu M, Wang Q, Zhang X, Bian H, Zhu P, Chen ZN: CD147 contributes to SARS-CoV-2-induced pulmonary fibrosis. *Signal Transduct Target Ther* 7(1): 382, 2022. DOI: 10.1038/s41392-022-01230-5
- 16 Sinha S, Castillo V, Espinoza CR, Tindle C, Fonseca AG, Dan JM, Katkar GD, Das S, Sahoo D, Ghosh P: COVID-19 lung disease shares driver AT2 cytopathic features with Idiopathic pulmonary fibrosis. *EBioMedicine* 82: 104185, 2022. DOI: 10.1016/j.ebiom.2022.104185
- 17 Kalash R, Epperly MW, Goff J, Dixon T, Sprachman MM, Zhang X, Shields D, Cao S, Franicola D, Wipf P, Berhane H, Wang H, Au J, Greenberger JS: Amelioration of radiation-induced pulmonary fibrosis by a water-soluble bifunctional sulfoxide radiation mitigator (MMS350). *Radiat Res* 180(5): 474-490, 2013. DOI: 10.1667/RR3233.1
- 18 Kalash R, Berhane H, Au J, Rhieu BH, Epperly MW, Goff J, Dixon T, Wang H, Zhang X, Franicola D, Shinde A, Greenberger JS: Differences in irradiated lung gene transcription between fibrosis-prone C57BL/6NHsd and fibrosis-resistant C3H/HeNHsd mice. *In Vivo* 28: 147-172, 2014.
- 19 Rios CI, Cassatt DR, Hollingsworth BA, Satyamitra MM, Tadesse YS, Taliaferro LP, Winters TA, DiCarlo AL: Commonalities between COVID-19 and radiation injury. *Radiat Res* 195(1): 1-24, 2021. DOI: 10.1667/RADE-20-00188.1
- 20 Prasanna PG, Woloschak GE, DiCarlo AL, Buchsbaum JC, Schaeue D, Chakravarti A, Cucinotta FA, Formenti SC, Guha C, Hu DJ, Khan MK, Kirsch DG, Krishnan S, Leitner WW, Marples B, McBride W, Mehta MP, Rafii S, Sharon E, Sullivan JM, Weichselbaum RR, Ahmed MM, Vikram B, Coleman CN, Held KD: Low-dose radiation therapy (LDRT) for COVID-19: Benefits or risks? *Radiat Res* 194(5): 452-464, 2020. DOI: 10.1667/RADE-20-00211.1
- 21 Kommos FKF, Schwab C, Tavernar L, Schreck J, Wagner WL, Merle U, Jonigk D, Schirmacher P, Longnerich T: The pathology of severe COVID-19-related lung damage. *Dtsch Arztebl Int* 117(29-30): 500-506, 2020. DOI: 10.3238/arztebl.2020.0500
- 22 Sadhukhan P, Ugurlu MT, Hoque MO: Effect of COVID-19 on lungs: focusing on prospective malignant phenotypes. *Cancers (Basel)* 12(12): 3822, 2020. DOI: 10.3390/cancers12123822
- 23 Budnevsky AV, Avdeev SN, Kosanovic D, Shishkina VV, Filin AA, Esaulenko DI, Ovsyannikov ES, Samoylenko TV, Redkin



- AN, Suvorova OA, Perveeva IM: Role of mast cells in the pathogenesis of severe lung damage in COVID-19 patients. *Respir Res* 23(1): 371, 2022. DOI: 10.1186/s12931-022-02284-3
- 24 Xu R, Feng Z, Wang FS: Mesenchymal stem cell treatment for COVID-19. *EBioMedicine* 77: 103920, 2022. DOI: 10.1016/j.ebiom.2022.103920
- 25 Ohgushi M, Ogo N, Yanagihara T, Harada Y, Sumida K, Egashira A, Asoh T, Maeyama T, Yoshizawa S: Tacrolimus treatment for post-COVID-19 interstitial lung disease. *Intern Med* 61(4): 585-589, 2022. DOI: 10.2169/internalmedicine.7971-21
- 26 Wang F, Kream RM, Stefano GB: Long-term respiratory and neurological sequelae of COVID-19. *Med Sci Monit* 26: e928996, 2020. DOI: 10.12659/MSM.928996
- 27 Bösmüller H, Matter M, Fend F, Tzankov A: The pulmonary pathology of COVID-19. *Virchows Arch* 478(1): 137-150, 2021. DOI: 10.1007/s00428-021-03053-1
- 28 Roden AC, Boland JM, Johnson TF, Aubry MC, Lo Y, Butt YM, Maleszewski JJ, Larsen BT, Tazelaar HD, Khor A, Smith ML, Moua T, Jenkins SM, Moyer AM, Yi ES, Bois MC: Late complications of COVID-19. *Arch Pathol Lab Med* 146(7): 791-804, 2022. DOI: 10.5858/arpa.2021-0519-SA
- 29 Koukourakis MI: Low-dose radiotherapy for late-stage COVID-19 pneumonia? *Dose Response* 18(3): 1559325820951357, 2020. DOI: 10.1177/1559325820951357
- 30 Brosnahan SB, Jonkman AH, Kugler MC, Munger JS, Kaufman DA: COVID-19 and respiratory system disorders: Current knowledge, future clinical and translational research questions. *Arterioscler Thromb Vasc Biol* 40(11): 2586-2597, 2020. DOI: 10.1161/ATVBAHA.120.314515
- 31 Tynecka M, Janucik A, Niemira M, Zbikowski A, Stocker N, Tarasik A, Starosz A, Grubczak K, Szalkowska A, Korotko U, Reszec J, Kwasniewski M, Kretowski A, Akdis C, Sokolowska M, Moniuszko M, Eljaszewicz A: The short-term and long-term effects of intranasal mesenchymal stem cell administration to noninflamed mice lung. *Front Immunol* 13: 967487, 2022. DOI: 10.3389/fimmu.2022.967487
- 32 Rogers CJ, Harman RJ, Minnell BA, Schreiber MA, Xiang C, Wang FS, Santidrian AF, Minev BR: Rationale for the clinical use of adipose-derived mesenchymal stem cells for COVID-19 patients. *J Transl Med* 18(1): 203, 2020. DOI: 10.1186/s12967-020-02380-2
- 33 You X, Jiang X, Zhang C, Jiang K, Zhao X, Guo T, Zhu X, Bao J, Dou H: Dihydroartemisinin attenuates pulmonary inflammation and fibrosis in rats by suppressing JAK2/STAT3 signaling. *Aging (Albany NY)* 14(3): 1110-1127, 2022. DOI: 10.18632/aging.203874
- 34 Susanto AD, Triyoga PA, Isbaniah F, Fairuz A, Cendikiawan H, Zaron F, Aryanti I, Irbah SN, Hidayat M: Lung fibrosis sequelae after recovery from COVID-19 infection. *J Infect Dev Ctries* 15(03): 360-365, 2021. DOI: 10.3855/jidc.13686
- 35 Cao J, Li L, Xiong L, Wang C, Chen Y, Zhang X: Research on the mechanism of berberine in the treatment of COVID-19 pneumonia pulmonary fibrosis using network pharmacology and molecular docking. *Phytomed Plus* 2(2): 100252, 2022. DOI: 10.1016/j.phyplu.2022.100252
- 36 Liu G, Philp AM, Corte T, Travis MA, Schilter H, Hansbro NG, Burns CJ, Eapen MS, Sohal SS, Burgess JK, Hansbro PM: Therapeutic targets in lung tissue remodelling and fibrosis. *Pharmacol Ther* 225: 107839, 2021. DOI: 10.1016/j.pharmthera.2021.107839
- 37 Ghebremedhin A, Salam AB, Adu-Addai B, Noonan S, Stratton R, Ahmed MSU, Khantwal C, Martin GR, Lin H, Andrews C, Karanam B, Rudloff U, Lopez H, Jaynes J, Yates C: A novel CD206 targeting peptide inhibits bleomycin-induced pulmonary fibrosis in mice. *Cells* 12(9): 1254, 2023. DOI: 10.3390/cells12091254
- 38 Zhang R, Tan Y, Yong C, Jiao Y, Tang X, Wang D: Pirfenidone ameliorates early pulmonary fibrosis in LPS-induced acute respiratory distress syndrome by inhibiting endothelial-to-mesenchymal transition *via* the Hedgehog signaling pathway. *Int Immunopharmacol* 109: 108805, 2022. DOI: 10.1016/j.intimp.2022.108805
- 39 Ture HY, Kim NR, Nam EJ: New-onset retroperitoneal fibrosis following COVID-19 mRNA vaccination: Coincidental or vaccine-induced phenomenon? *Int J of Rheum Dis* 26(7): 1368-1372, 2023. DOI: 10.1111/1756-185X.14621
- 40 Bharat A, Querrey M, Markov NS, Kim S, Kurihara C, Garza-Castillon R, Manerikar A, Shilatifard A, Tomic R, Politanska Y, Abdala-Valencia H, Yeldandi AV, Lomasney JW, Misharin AV, Budinger GRS: Lung transplantation for patients with severe COVID-19. *Sci Transl Med* 12(574): eabe4282, 2020. DOI: 10.1126/scitranslmed.abe4282
- 41 Micheletto C, Izquierdo JL, Avdeev SN, Escobar RAR, Gallego MCP: N-Acetylcysteine as a therapeutic approach to post-COVID-19 pulmonary fibrosis adjunctive treatment. *Eur Rev Med Pharmacol Sci* 26(13): 4872-4880, 2022. DOI: 10.26355/eurev\_202207\_29212
- 42 Sakızci Uyar B, Ensarioğlu K, Kurt EB, Özkan D, Özbal Güneş S: Anti-fibrotic treatment for pulmonary fibrosis induced by COVID-19: a case presentation. *Turk J Anaesthesiol Reanim* 50(3): 228-231, 2022. DOI: 10.5152/TJAR.2021.20450
- 43 Zhao Y, Yan Z, Liu Y, Zhang Y, Shi J, Li J, Ji F: Effectivity of mesenchymal stem cells for bleomycin-induced pulmonary fibrosis: a systematic review and implication for clinical application. *Stem Cell Res Ther* 12(1): 470, 2021. DOI: 10.1186/s13287-021-02551-y
- 44 Zhong H, Zhou Y, Mei SY, Tang R, Feng JH, He ZY, Xu QY, Xing SP: Scars of COVID-19: A bibliometric analysis of post-COVID-19 fibrosis. *Front Public Health* 10: 967829, 2022. DOI: 10.3389/fpubh.2022.967829
- 45 Zhang C, Wu Z, Li JW, Tan K, Yang W, Zhao H, Wang GQ: Discharge may not be the end of treatment: Pay attention to pulmonary fibrosis caused by severe COVID-19. *J Med Virol* 93(3): 1378-1386, 2021. DOI: 10.1002/jmv.26634
- 46 Wang Y, Sang X, Shao R, Qin H, Chen X, Xue Z, Li L, Wang Y, Zhu Y, Chang Y, Gao X, Zhang B, Zhang H, Yang J: Xuanfei Baidu Decoction protects against macrophages induced inflammation and pulmonary fibrosis *via* inhibiting IL-6/STAT3 signaling pathway. *J Ethnopharmacol* 283: 114701, 2022. DOI: 10.1016/j.jep.2021.114701
- 47 Wang Y, Zhang L, Wu GR, Zhou Q, Yue H, Rao LZ, Yuan T, Mo B, Wang FX, Chen LM, Sun F, Song J, Xiong F, Zhang S, Yu Q, Yang P, Xu Y, Zhao J, Zhang H, Xiong W, Wang CY: MBD2 serves as a viable target against pulmonary fibrosis by inhibiting macrophage M2 program. *Sci Adv* 7(1): eabb6075, 2021. DOI: 10.1126/sciadv.abb6075
- 48 Kanvinde S, Deodhar S, Kulkarni TA, Jogdeo CM: Nanotherapeutic approaches to treat COVID-19-induced pulmonary fibrosis. *BioTech (Basel)* 12(2): 34, 2023. DOI: 10.3390/biotech12020034

- 49 Huang WJ, Tang XX: Virus infection induced pulmonary fibrosis. *J Transl Med* 19(1): 496, 2021. DOI: 10.1186/s12967-021-03159-9
- 50 Cui Y, Xin H, Tao Y, Mei L, Wang Z: *Arenaria kansuensis* attenuates pulmonary fibrosis in mice *via* the activation of Nrf2 pathway and the inhibition of NF- $\kappa$ B/TGF- $\beta$ 1/Smad2/3 pathway. *Phytother Res* 35(2): 974-986, 2021. DOI: 10.1002/ptr.6857
- 51 Sheng H, Lin G, Zhao S, Li W, Zhang Z, Zhang W, Yun L, Yan X, Hu H: Antifibrotic mechanism of piceatannol in bleomycin-induced pulmonary fibrosis in mice. *Front Pharmacol* 13: 771031, 2022. DOI: 10.3389/fphar.2022.771031
- 52 Rumende CM, Susanto EC, Sitorus TP: The management of pulmonary fibrosis in COVID-19. *Acta Med Indones* 53(2): 233-241, 2021.
- 53 Kiener M, Roldan N, Machahua C, Sengupta A, Geiser T, Guenat OT, Funke-Chambour M, Hobi N, Kruthof-de Julio M: Human-based advanced *in vitro* approaches to investigate lung fibrosis and pulmonary effects of COVID-19. *Front Med (Lausanne)* 8: 644678, 2021. DOI: 10.3389/fmed.2021.644678
- 54 Islam MA, Versypt ANF: Mathematical modeling of impacts of patient differences on COVID-19 lung fibrosis outcomes. *bioRxiv*, 2022. DOI: 10.1101/2022.11.06.515367
- 55 Stojanovic D, Stojanovic M, Milenkovic J, Velickov A, Ignjatovic A, Milojkovic M: Renalase challenges the oxidative stress and fibroproliferative response in COVID-19. *Oxid Med Cell Longev* 2022: 4032704, 2022. DOI: 10.1155/2022/4032704
- 56 Schmitt CA, Tchkonja T, Niedernhofer LJ, Robbins PD, Kirkland JL, Lee S: COVID-19 and cellular senescence. *Nat Rev Immunol* 23(4): 251-263, 2023. DOI: 10.1038/s41577-022-00785-2
- 57 D'Agnillo F, Walters K-A, Xiao Y, Sheng Z-M, Scherler K, Park J, Gygli S, Rosas LA, Sadtler K, Kalish H, Blatt, III CA, Zhu R, Gatzke L, Bushell C, Memoli MJ, O'Day SJ, Fischer TD, Hammond TC, Lee RC, Cash JC, Powers ME, O'Keefe GE, Butnor KJ, Rapkiewicz AV, Travis WD, Layne SP, Kash JC, Taubenberger JK: Lung epithelial and endothelial damage, loss of tissue repair, inhibition of fibrinolysis, and cellular senescence in fatal COVID-19. *Sci Transl Med* 13(620): eabj7790, 2021. DOI: 10.1126/scitranslmed.abj7790
- 58 Hong X, Wang L, Zhang K, Liu J, Liu JP: Molecular mechanisms of alveolar epithelial stem cell senescence and senescence-associated differentiation disorders in pulmonary fibrosis. *Cells* 11(5): 877, 2022. DOI: 10.3390/cells11050877
- 59 Mukherjee A, Epperly MW, Shields D, Hou W, Fisher R, Hamade D, Wang H, Saiful Huq M, Bao R, Tabib T, Monier D, Watkins S, Calderon M, Greenberger JS: Ionizing irradiation-induced F $\gamma$ r in senescent cells mediates fibrosis. *Cell Death Discov* 7(1): 349, 2021. DOI: 10.1038/s41420-021-00741-4
- 60 Mukherjee A, Epperly MW, Fisher R, Hou W, Shields D, Saiful Huq M, Pifer PM, Mulherkar R, Wilhite TJ, Wang H, Wipf P, Greenberger JS: Inhibition of tyrosine kinase F $\gamma$ r prevents radiation-induced pulmonary fibrosis (RIPF). *Cell Death Discov* 9(1): 252, 2023. DOI: 10.1038/s41420-023-01538-3
- 61 Sivananthan A, Shields D, Fisher R, Hou W, Zhang X, Francicola D, Epperly MW, Wipf P, Greenberger JS: Continuous one year oral administration of the radiation mitigator, MMS350, after total-body irradiation, restores bone marrow stromal cell proliferative capacity and reduces senescence in Fanconi anemia (Fanc $\alpha$ (-/-)) mice. *Radiat Res* 191(2): 139-153, 2019. DOI: 10.1667/RR15199.1
- 62 McCray PB Jr, Pewe L, Wohlford-Lenane C, Hickey M, Manzel L, Shi L, Netland J, Jia HP, Halabi C, Sigmund CD, Meyerholz DK, Kirby P, Look DC, Perlman S: Lethal infection of K18-hACE2 mice infected with severe acute respiratory syndrome coronavirus. *J Virol* 81(2): 813-821, 2007. DOI: 10.1128/JVI.02012-06
- 63 Manni ML, Oury TD: Oxidative stress and pulmonary fibrosis. In: *Systems Biology of Free Radicals and Antioxidants*. Laher I (ed.). Berlin, Germany, Springer, pp. 1611-1631, 2014.
- 64 Steinman J, Epperly M, Hou W, Willis J, Wang H, Fisher R, Liu B, Bahar I, McCaw T, Kagan V, Bayir H, Yu J, Wipf P, Li S, Huq MS, Greenberger JS: Improved total-body irradiation survival by delivery of two radiation mitigators that target distinct cell death pathways. *Radiat Res* 189(1): 68-83, 2018. DOI: 10.1667/RR14787.1
- 65 Thermozier S, Hou W, Zhang X, Shields D, Fisher R, Bayir H, Kagan V, Yu J, Liu B, Bahar I, Epperly MW, Wipf P, Wang H, Huq MS, Greenberger JS: Anti-ferroptosis drug enhances total-body irradiation mitigation by drugs that block apoptosis and necroptosis. *Radiat Res* 193(5): 435-450, 2020. DOI: 10.1667/RR15486.1
- 66 Epperly M, Bray J, Kraeger S, Zwacka R, Engelhardt J, Travis E, Greenberger J: Prevention of late effects of irradiation lung damage by manganese superoxide dismutase gene therapy. *Gene Ther* 5(2): 196-208, 1998. DOI: 10.1038/sj.gt.3300580
- 67 Epperly MW, Travis EL, Sikora C, Greenberger JS: Manganese [correction of Magnesium] superoxide dismutase (MnSOD) plasmid/liposome pulmonary radioprotective gene therapy: modulation of irradiation-induced mRNA for IL-1, TNF- $\alpha$ , and TGF- $\beta$  correlates with delay of organizing alveolitis/fibrosis. *Biol Blood Marrow Transpl* 5: 204-214, 1999. DOI: 10.1053/bbmt.1999.v5.pm10465100
- 68 Li Y, Dong S, Tamaskar A, Wang H, Zhao J, Ma H, Zhao Y: Proteasome inhibitors diminish c-Met expression and induce cell death in non-small cell lung cancer cells. *Oncol Res* 28(5): 497-507, 2020. DOI: 10.3727/096504020X15929939001042
- 69 Epperly MW, Guo HL, Jefferson M, Nie S, Gretton J, Bernarding M, Bar-sagi D, Archer H, Greenberger JS: Cell phenotype specific kinetics of expression of intratracheally injected manganese superoxide dismutase-plasmid/liposomes (MnSOD-PL) during lung radioprotective gene therapy. *Gene Ther* 10(2): 163-171, 2003. DOI: 10.1038/sj.gt.3301852
- 70 Epperly MW, Guo H, Gretton JE, Greenberger JS: Bone marrow origin of myofibroblasts in irradiation pulmonary fibrosis. *Am J Resp Mol Cell Biol* 29(2): 213-224, 2003. DOI: 10.1165/rcmb.2002-0069OC
- 71 Rodríguez A, Epperly M, Filiatrault J, Velázquez M, Yang C, McQueen K, Sambel LA, Nguyen H, Iyer DR, Juárez U, Ayala-Zambrano C, Martignetti DB, Frías S, Fisher R, Parmar K, Greenberger JS, D'Andrea AD: TGF $\beta$  pathway is required for viable gestation of Fanconi anemia embryos. *PLoS Genet* 18(11): e1010459, 2022. DOI: 10.1371/journal.pgen.1010459
- 72 Sprachman MM, Wipf P: A bifunctional dimethylsulfoxide substitute enhances the aqueous solubility of small organic molecules. *Assay Drug Dev Technol* 10(3): 269-277, 2012. DOI: 10.1089/adt.2011.0421
- 73 Shang J, Ye G, Shi K, Wan Y, Luo C, Aihara H, Geng Q, Auerbach A, Li F: Structural basis of receptor recognition by SARS-CoV-2. *Nature* 581(7807): 221-224, 2020. DOI: 10.1038/s41586-020-2179-y

- 74 Lan J, Ge J, Yu J, Shan S, Zhou H, Fan S, Zhang Q, Shi X, Wang Q, Zhang L, Wang X: Structure of the SARS-CoV-2 spike receptor-binding domain bound to the ACE2 receptor. *Nature* 581(7807): 215-220, 2020. DOI: 10.1038/s41586-020-2180-5
- 75 Yuan M, Wu NC, Zhu X, Lee CD, So RTY, Lv H, Mok CKP, Wilson IA: A highly conserved cryptic epitope in the receptor binding domains of SARS-CoV-2 and SARS-CoV. *Science* 368(6491): 630-633, 2020. DOI: 10.1126/science.abb7269
- 76 Soysouvanh F, Benadjaoud MA, Dos Santos M, Mondini M, Lavigne J, Bertho A, Buard V, Tarlet G, Adnot S, Deutsch E, Guipaud O, Paget V, François A, Milliat F: Stereotactic lung irradiation in mice promotes long-term senescence and lung injury. *Int J Radiat Oncol Biol Phys* 106(5): 1017-1027, 2020. DOI: 10.1016/j.ijrobp.2019.12.039
- 77 Manning CM, Johnston CJ, Reed CK, Lawrence BP, Williams JP, Finkelstein JN: Lung irradiation increases mortality after influenza A virus challenge occurring late after exposure. *Int J Radiat Oncol Biol Phys* 86(1): 128-135, 2013. DOI: 10.1016/j.ijrobp.2012.10.019
- 78 Li N, Parrish M, Chan TK, Yin L, Rai P, Yoshiyuki Y, Abolhassani N, Tan KB, Kiraly O, Chow VT, Engelward BP: Influenza infection induces host DNA damage and dynamic DNA damage responses during tissue regeneration. *Cell Mol Life Sci* 72(15): 2973-2988, 2015. DOI: 10.1007/s00018-015-1879-1
- 79 Sargiacomo C, Sotgia F, Lisanti MP: COVID-19 and chronological aging: senolytics and other anti-aging drugs for the treatment or prevention of corona virus infection? *Aging (Albany NY)* 12(8): 6511-6517, 2020. DOI: 10.18632/aging.103001
- 80 Tabasso AFS, Jones DJL, Jones GDD, Macip S: Radiotherapy-induced senescence and its effects on responses to treatment. *Clinical Oncology* 31(5): 283-289, 2019. DOI: 10.1016/j.clon.2019.02.003
- 81 Liu RM, Liu G: Cell senescence and fibrotic lung diseases. *Exp Gerontol* 132: 110836, 2020. DOI: 10.1016/j.exger.2020.110836
- 82 Wiley CD, Brumwell AN, Davis SS, Jackson JR, Valdovinos A, Calhoun C, Alimirah F, Castellanos CA, Ruan R, Wei Y, Chapman HA, Ramanathan A, Campisi J, Jourdan Le Saux C: Secretion of leukotrienes by senescent lung fibroblasts promotes pulmonary fibrosis. *JCI Insight* 4(24): e130056, 2019. DOI: 10.1172/jci.insight.130056
- 83 Basisty N, Kale A, Jeon OH, Kuehnemann C, Payne T, Rao C, Holtz A, Shah S, Sharma V, Ferrucci L, Campisi J, Schilling B: A proteomic atlas of senescence-associated secretomes for aging biomarker development. *PLoS Biol* 18(1): e3000599, 2020. DOI: 10.1371/journal.pbio.3000599
- 84 Schafer MJ, Haak AJ, Tschumperlin DJ, LeBrasseur NK: Targeting senescent cells in fibrosis: pathology, paradox, and practical considerations. *Curr Rheumatol Rep* 20(1): 3, 2018. DOI: 10.1007/s11926-018-0712-x
- 85 Rwigema JC, Beck B, Wang W, Doemling A, Epperly MW, Shields D, Goff JP, Franicola D, Dixon T, Frantz MC, Wipf P, Tyurina Y, Kagan VE, Wang H, Greenberger JS: Two strategies for the development of mitochondrion-targeted small molecule radiation damage mitigators. *Int J Radiat Oncol Biol Phys* 80(3): 860-868, 2011. DOI: 10.1016/j.ijrobp.2011.01.059
- 86 Blanco-Melo D, Nilsson-Payant BE, Liu WC, Uhl S, Hoagland D, Møller R, Jordan TX, Oishi K, Panis M, Sachs D, Wang TT, Schwartz RE, Lim JK, Albrecht RA, tenOever BR: Imbalanced host response to SARS-CoV-2 drives development of COVID-19. *Cell* 181(5): 1036-1045.e9, 2020. DOI: 10.1016/j.cell.2020.04.026

*Received November 14, 2023*

*Revised March 4, 2024*

*Accepted March 19, 2024*